Knots in plasma

Smiet, C.B.

1

Introduction

Knots are meant to securely and stably fasten and connect. This is true in the literal sense, where knots secure boats to piers and shoes to feet, as well as in the figurative sense where 'to tie a knot' signifies the creation of a near unbreakable bond, linking two people into a stable and inseparable unity. Their remarkable stability led Lord Kelvin to speculate that atoms themselves consisted of vortex knots in the æther [1]. In recent years the application of knot theory to physical phenomena has experienced a true revival with knotted structures being described in field theories [2,3], liquid crystals [4,5] superconductors and superfluids [6,7], Bose-Einstein condensates [8,9] and molecular biology [10].

In plasma physics the connection between knots and stability has been established since 1969 when Moffatt discovered that the conserved quantity identified by Woltjer [11] was in fact a measure of the linking and knotting of magnetic field lines [12]. The conservation of this quantity in fluid dynamics was discovered independently in 1966 by Steenbeck Krause and Rädler [13] and named 'Schraubensinn', but due to the linguistic and geopolitical barriers of the time this quantity is now known by the name given to it by Moffatt: helicity. Magnetic helicity is a measure of the average linking of field lines in a configuration and reduces to the Gauss linking integral calculated over every pair of field lines [14]. This was made mathematically rigorous by the concept of the asymptotic Hopf invariant introduced by Arnold [15].

Because of the importance of linking and knottedness to plasma dynamics a large body of research is devoted to topological aspects of magnetic fields in plasma. The topology of the linked or knotted field can be used to define a unique knot energy in ideal, incompressible MHD [16]. Kamchatnov used the knotted structure of the Hopf map to construct analytical solutions to the ideal MHD equations [17], later expanded on by

Sagdeev [18]. This same structure was used to generate knotted solutions to Maxwell's equations [19,20]. Based on this, solutions of Maxwell's equations were constructed where all field lines are torus knots [21], and where the field lines lie on linked torus-knotted surfaces [22]. The torus knotted fields have again been used to construct ideal MHD solitons [23]. Recently a new analytical technique has been described by Kedia with which a magnetic field of arbitrary helicity and well-defined knotting of field lines can be constructed [24].

This thesis addresses the question how helicity in a localized magnetic field provides stability to a plasma. We show, using different numerical schemes and different initial conditions that the initial helicity is translated to a self-organized localized magnetic equilibrium where field lines lie on nested toroidal surfaces. The tendency of the localized magnetic field to expand is countered by an external pressure, and a toroidal depression in pressure is realized with a minimum in pressure on the magnetic axis of the structure.

We found this solution by explicitly looking for a structure like this: when several Hopf-linked rings resistively reconnect they give rise to a magnetic field which is topologically similar to the full Hopf structure. What turned out to be remarkable is that these dynamics are more universal: not only linked flux rings reconfigure to such an equilibrium, but also trefoil knotted tubes, single twisted tubes and any other magnetic field containing helicity. With hindsight these structures are also seen in numerical simulations that predate this research. The nonhelical configuration of Borromean linked flux tubes presented in [25] gives rise to two such equilibria of opposite helicity, and the radio bubbles described by Braithwaite [26] carry a similar magnetic topology.

These structures are intrinsically stable, and in essence the opposite of the configuration achieved in a tokamak. To first order the design of a tokamak should give rise to an equilibrium. However it turns out that this equilibrium is unstable, leading to chaotic plasma dynamics. Fighting these chaotic dynamics is the main challenge in fusion reactor designs. Our results indicate that instead of trying to balance the unstable equilibrium, a configuration with a lowered pressure on the magnetic axis can be intrinsically stable.

The magnetic topology considered in chapters 2, 3 and 5 of this thesis is similar to the fields in novel fusion reactor designs such as the self-organized fields in the Tri Alpha experiment [27] and the General Fusion reactor. The results of this thesis can be used to better understand instabilities plasma experiments as well as guide the design of new plasma experiments where this magnetic equilibrium is achieved. The near universality of the appearance of this structure in numerical simulations would also suggest that such an equilibrium could occur in an astrophysical context. Numerical studies by Braithwaite on radio bubbles ejected from active galactic nuclei show similar structures on a galactic scale [26]. Coronal mass ejections throw large amounts of plasma with linked field lines into the interplanetary medium where it subsequently relaxes. Structures referred to as magnetic clouds could consist of a similar magnetic equilibrium, but more research is

needed to confirm this.

This introduction chapter will give a brief overview of plasma physics in section 1.1. The mathematical models used do describe the plasma dynamics are given in section 1.2. Section 1.3 describes the equations solved by the numerical scheme used in most of this thesis, and section 1.4 gives more detail on the concept of magnetic helicity and its topological interpretation. In section 1.5 we describe the Hopf map, and how to construct a magnetic field from it.

1.1 The plasma universe

We live in a plasma filled universe. This might not seem obvious at first sight, since most objects we interact with on a daily basis are all either liquid, solid or gaseous. It is for this reason that our understanding of plasma as a state of matter is a relatively recent development. But if we take a step back and look at our entire universe, then we see that our planet is one of only a sparse collection of rocks floating around in which matter has been able to organize into the familiar states. In fact, only about 5 percent of the baryonic (ordinary) matter in the universe* exists in one of these three well-understood states. Of the rest of the baryonic matter in the universe, much is contained in stars, large spheres of plasma where hydrogen is fused releasing energy. In the space between the stars there is also matter to be found. Most of this sparsely distributed matter is ionized, and on a large enough scale the interplanetary, interstellar, and even intergalactic medium behaves as a plasma.

Plasma as a state of matter has many interesting properties. It behaves as a fluid, free to flow and swirl in complicated patterns described by hydrodynamics. But there is an additional property of plasma that makes its description even more complicated than the already significantly complex laws governing fluids. Plasmas are ionized, the ordered structure of electrons bound to atoms has been broken up, and the state consists of freely moving charged particles. The moving charged particles are able to create large magnetic fields, resulting in long-range interactions within the fluid. Because of the importance of these magnetic fields, the study of the dynamics of magnetized plasma is called magnetohydrodynamics (MHD).†

In this thesis we are concerned with the class of plasma where the magnetic field significantly affects the plasma structure and behaviour. This regime is found throughout the universe, in the centers of fusing stars, and in coronal loops, the beautiful wisps of

* Here we are discounting dark matter and dark energy, which is estimated to compose about 95 percent of all mass in the universe. No sensible statement can be made as to in what state dark matter exists.

† The name plasma originally comes from medicine, where it is used to signify the clear fluid that remains when the cells have been removed from blood. It was Irving Langmuir, one of the first plasma physicists, who proposed that an ionized gas could similarly be seen as a fluid which entrained the charged ions and electrons, and named that medium plasma. This turned out to be false. However the name stuck, and ever since plasma physicists have had to explain that their work has noting to do with blood.

Figure 1.1: Vincent van Gogh beautifully captured the turbulent dynamics present in interstellar plasma long before their mathematical description could be elucidated.

plasma that reach out from the surface into the thin, hot plasma just outside stars. On galactic scales, spread out magnetic fields subtly influence the motion of galaxies.

The importance of magnetic fields on the behaviour of plasma allows us to approach it from a very interesting perspective: knot theory. Magnetic field lines (integral curves of the magnetic field) are curves in the three-dimensional volume of a plasma. Since these curves cannot start or end in free space*, they often close on themselves, and thus are a physical manifestation of the embedding of a circle in three-dimensional space, i.e. they form a knot. Looking at the magnetic field in a plasma from this perspective is given more credence by a beautiful discovery made by Moffatt [12] (see also section 1.4): The linking and knotting of magnetic field lines in an ideal plasma is conserved! If a magnetic field line starts out knotted, the plasma dynamics will not be able to undo that knot.

Here on earth the promise of unlimited clean energy has driven much of plasma research. Almost all of the energy used here on earth comes from the sun in one form or another, where it is produced by the thermonuclear fusion of ions in the solar core. This reaction happens extremely slow, and only at extreme temperatures where the thermal motion of the ions is high enough to force the nuclei together to fuse into more stable configurations. Since there is an abundance of light elements here on earth, the goal is to develop a fusion reactor where a plasma can be kept in place whilst it is heated to a sufficiently high temperature to undergo these reactions, in other words, to put the sun in a bottle.

* Except for a zero measure subset of the field lines.

1.2 The mathematical description of plasma

In this thesis we limit ourselves to two of the simplest mathematical descriptions of plasma: Ideal magnetohydrodynamics (MHD) and resistive magnetohydrodynamics. There are many more complex descriptions of a plasma, such as two-fluid, gyrokinetics, or the fully-kinetic Vlasov equation [28]. These models are used to describe with high accuracy the effects going on in modern fusion reactors, but they are all refinements, and they reduce to the MHD equations.

In order to simplify the notation, in this thesis we will always use natural units such that $\epsilon_0 = \mu_0 = c = 1$.

1.2.1 Ideal MHD

Ideal magnetohydrodynamics (IMHD) describes plasma as a perfectly conducting fluid. In the systems we consider the fluid is either incompressible, or density and pressure are linearly related. In order to fully describe the state of this fluid, we then need three or four variables; the fluid velocity $\boldsymbol{v}$, the magnetic field $\boldsymbol{B}$, a density ρ (compressible IMHD), and pressure p (incompressible IMHD).

Let us first consider the evolution of the fluid velocity. This is directly inferred from Newtons equation $\boldsymbol{F} = m\boldsymbol{a}$, where the fluid acceleration is caused by the forces acting on the plasma. These forces are the Lorentz force, $\boldsymbol{j} \times \boldsymbol{B}$, and the force resultant from a gradient in pressure ∇p such that we have:

$$\rho \left(\frac{\partial \boldsymbol{v}}{\partial t} + \boldsymbol{v} \cdot \nabla \boldsymbol{v} \right) = -\nabla p + \boldsymbol{j} \times \boldsymbol{B}. \tag{1.1}$$

For astrophysical applications it is often important to also include a gravitational term in equation (1.1). In this thesis we will neglect gravitational effects.

This equation uses the current density $\boldsymbol{j}$, but the current density is not an independent variable. It can be written in terms of the magnetic field, using the fourth Maxwell equation: $\nabla \times \boldsymbol{B} = \boldsymbol{j} + \frac{\partial \boldsymbol{E}}{\partial t}$. Since we are considering a perfectly conducting fluid, the displacement current $\frac{\partial \boldsymbol{E}}{\partial t}$ is zero. This gives us the Ampère law:

$$\nabla \times \boldsymbol{B} = \boldsymbol{j}. \tag{1.2}$$

Additionally we need to take into account how the magnetic field changes in an ideal fluid. This can be inferred from the third Maxwell equation $\frac{\partial \boldsymbol{B}}{\partial t} = -\nabla \times \boldsymbol{E}$. Consider what the electric field would be in a perfectly conducting fluid. If that fluid is not in motion, there can be no electric field at all, as all charge imbalance would equilibrate. But if the fluid is moving through a magnetic field the Lorentz force will push positive charges to one side, and negative charges to the other side of the conductor, giving rise to an electric

field. This is mathematically expressed as Gallilean transform on the electric field. This gives rise to an electric field perpendicular to both the fluid velocity and magnetic field, $\boldsymbol{E} = -\boldsymbol{v} \times \boldsymbol{B}$. The equation for the time evolution of the magnetic field then becomes

$$\frac{\partial \boldsymbol{B}}{\partial t} = \nabla \times (\boldsymbol{v} \times \boldsymbol{B}). \tag{1.3}$$

Another way of describing the above equation is "field lines go with the flow", and it is this equation that we shall see is responsible for the conservation of magnetic topology and helicity discussed in the next section.

There is one additional constraint to consider when describing a magnetic field, which is the solenoidal condition

$$\nabla \cdot \boldsymbol{B} = 0. \tag{1.4}$$

If this condition is true at any time t, equation (1.3) guarantees it will hold true at any later time.

In incompressible ideal MHD, the fluid velocity field also follows the solenoidal condition, $\nabla \cdot \boldsymbol{v} = 0$.

When considering compressible MHD, we will assume an isothermal plasma. The density is then given by the continuity equation.

$$\frac{\partial \rho}{\partial t} = -\nabla \cdot \rho \boldsymbol{v}. \tag{1.5}$$

This equation implies that any change in mass must be caused by a corresponding flow through the boundary.

The pressure for a isothermal plasma is given by $p = c_s^2 \rho$ where the proportionality constant c_s^2 is the isothermal sound speed.

1.2.2 Compressible, viscous, resistive and isothermal MHD

Ideal MHD is a good approximation for a plasma, but many of the most interesting effects happen when a small amount of resistivity and viscosity is taken into account. The small resistivity allows for many new phenomena to occur which cannot occur in ideal MHD.

The momentum equation needs to be modified to incorporate the viscous forces, so equation (1.1) becomes:

$$\rho \left(\frac{\partial \boldsymbol{v}}{\partial t} + \boldsymbol{v} \cdot \nabla \boldsymbol{v} \right) = -\nabla p + \boldsymbol{j} \times \boldsymbol{B} + \boldsymbol{F}_{\text{visc}} \tag{1.6}$$

These viscous forces $\boldsymbol{F}_{\text{visc}}$ are anisotropic, but for simplicity and analytical tractability a scalar kinematic viscosity term ν can be assumed, such that the viscous force has the

following form:

$$\boldsymbol{F}_{\text{visc}} = \rho\nu\nabla^2\boldsymbol{v}. \tag{1.7}$$

The induction equation is also modified by the effects of resistivity. This induces an additional electric field in the direction of the current $\boldsymbol{E}_{\text{res}} = \eta\boldsymbol{j}$. The resistive induction equation then becomes:

$$\frac{\partial \boldsymbol{B}}{\partial t} = \nabla \times (\boldsymbol{v} \times \boldsymbol{B}) - \nabla \times \eta(\nabla \times \boldsymbol{B}) = \nabla \times (\boldsymbol{v} \times \boldsymbol{B}) + \eta\nabla^2\boldsymbol{B}, \tag{1.8}$$

where the last equality was derived assuming a spatially constant resistivity. Because of the form in which η appears in this equation, it is also called magnetic diffusivity.

To round out this set of equations we need to prescribe how the pressure and density change in time. In any physical system mass is conserved, thus any matter flowing into or out of a region must result in a change in the density. This results in the same continuity equation as in the ideal case:

$$\frac{\partial \rho}{\partial t} = -\nabla \cdot \rho\boldsymbol{v}. \tag{1.9}$$

A useful approximation is to assume an isothermal gas such that pressure and density are linearly related through the ideal gas law. Pressure then becomes linearly dependent on density:

$$p = \rho c_s^2. \tag{1.10}$$

Together equations (1.6) (1.8) (1.9) and (1.10) form a closed set of equations from which the full evolution of the fields can be calculated.

1.2.3 On the Lorentz force

The Lorentz force, $\mathbf{F}_{\text{L}} = \boldsymbol{j} \times \boldsymbol{B}$, is an important force that shapes a plasma and in this section we take a look at how to interpret this force. Since $\boldsymbol{j} = \nabla \times \boldsymbol{B}$, we can use the vector calculus identity $\nabla(\boldsymbol{a} \cdot \boldsymbol{b}) = (\boldsymbol{a} \cdot \nabla)\boldsymbol{b} + (\boldsymbol{b} \cdot \nabla)\boldsymbol{a} + \boldsymbol{a} \times (\nabla \times \boldsymbol{b}) + \boldsymbol{b} \times (\nabla \times \boldsymbol{a})$ to re-write it to:

$$(\nabla \times \boldsymbol{B}) \times \boldsymbol{B} = -\frac{1}{2}\nabla B^2 + \boldsymbol{B} \cdot \nabla\boldsymbol{B}. \tag{1.11}$$

By re-writing it in this way, we see that the Lorentz force has two components. The first term, $-\nabla B^2/2$, is commonly referred to as magnetic pressure. The magnetic pressure gives rise to a force directed from a region of high magnetic field strength towards a region of lower magnetic field strength.

The second component, $\boldsymbol{B} \cdot \nabla\boldsymbol{B}$ is called the magnetic tension force. This is because the effect of this force can be seen as the result of a tension in the magnetic field lines:

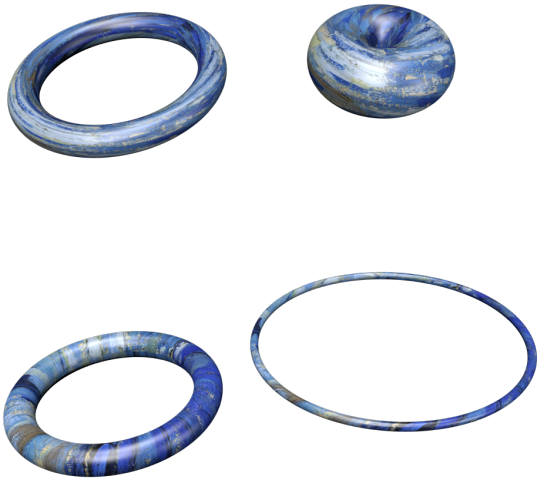

Figure 1.2: A magnetic flux tube whose field lines are in the direction of the ring will experience magnetic forces that pull the ring together and thicken it (top). When the magnetic field is around the short direction of the ring, the magnetic forces make the magnetic ring expand and thin (bottom).

as if the field lines were ropes that were pulled tight. Where the field lines are bent, this force gives rise to a straightening and restoring force.

Using this we can understand how simple magnetic configurations are shaped by these forces. Imagine a magnetic flux ring, where all field lines are directed along the ring, and the magnetic field is zero outside the ring. The magnetic pressure force will be directed outwards from the ring surface, causing the ring to fatten. At the same time the magnetic tension is pulling along the field lines, and will cause the ring to contract, to become a shorter. The net effect is that a ring of magnetic field fattens and shortens, going from a 'bicycle tire' to a 'truck tire'.

If the magnetic field is around the short direction of the ring, the opposite would happen. The magnetic tension would squeeze the ring tight, whilst the magnetic pressure would press it further out. The configuration would go from a 'truck tire" to a 'bicycle tire'. Note that such a magnetic field is set up by a current flowing along the ring, so another way to phrase this is to say that magnetic rings contract, and current rings expand. This process is illustrated in figure 1.2.

1.2.4 further enhancements

The work presented in this thesis is based on the above two descriptions of a plasma, either ideal MHD or isothermal resistive and viscous MHD. However a whole host of more elaborate and precise models of plasma dynamics exists. In this section we quantitatively describe these models, and some of the effects that they lead to which are not included in the above models.

One major limitation of MHD is that it treats the plasma as a single fluid with a given density. The fluid velocity $\boldsymbol{v}$ thus represents the average motion of all the particles, and the plasma remains effectively neutrally charged. In reality a plasma consists of positively charged ions and negatively charged electrons, which are free to move independently of one another. The mass of the electrons is three orders of magnitude less than the mass of the ions, which causes them to react on a different timescale. The difference in electron and ion motion can lead to charge separation, setting up large electric fields in the plasma. In order to take these effects into account one can use the **two-fluid model of MHD**, where the ions and electrons are modeled as two separate fluids. Two-fluid MHD is necessary to understand effects present in tokamaks such as the bootstrap current, a large current around the tokamak that is set up due to electric fields caused by differences in the distribution of the positive and negative charged species.

The two-fluid model still treats the plasma as two separate fluids, one positive and one negatively charged. This description as a fluid is only valid if there is enough interaction between the particles constituting the plasma that this reduction to the average motion holds. In extremely hot plasma and in very low density plasma the electrons and ions hardly interact with each other, and their mean free path can become large. It is then that **kinetic MHD** or its slightly simplified brother **gyrokinetic MHD** needs to be used. These models specify at every point in space a particle distribution function $f_i(\boldsymbol{r}, \boldsymbol{v})$ for both the ions and the electrons.

Kinetic MHD models are necessary to describe how highly energetic particles produced in fusion reactions redistribute their energy through the plasma. Another phenomenon that can only be described in kinetic theory and not in the simpler models is the occurrence of banana orbits. In a plasma the ions and electrons move with a generally high velocity along magnetic field lines. Up to first order the motion along the field line is unimpeded, but the velocity perpendicular to the magnetic field is affected by the Lorentz force, causing the particles to move in a tight spiral around the magnetic field lines. When such a particle moves along the field towards a region of higher field strength, the radius of this spiral becomes smaller, but since its angular momentum is conserved, the perpendicular velocity must increase. This causes the parallel velocity to decrease, and if the magnetic field strength increases enough, the particle is reflected away from the region of high field.

In a tokamak, or on any field line dense in a toroidal surface, the magnetic field

strength is higher on the inside of the torus than on the outside, because the same amount of toroidal flux needs to be distributed over a much larger area. There is therefore a subset of particles with low kinetic energy that are stuck on the outside of the torus, reflecting back and forth between the region of highest field strength in the center, effectively tracing out a banana shaped orbit. This subset of particles needs to be taken into account to accurately predict the magnetic field and disturbances that affect a tokamak plasma.

All these effects could also play a role in the magnetic configurations discussed in this thesis. The size of these effects are however small, and they do not fundamentally alter the equilibrium achieved. Future work should however look into this, as predictions from a kinetic model could show tell-tale signatures in particle energy distribution that could help identify structures.

1.3 Numerical methods

The coupled set of differential equations describing a plasma are rather hard to solve analytically. In fact, only in very simplified geometries, or by making use of reduced dimensionality or exploiting a symmetry, can analytical solutions be found.

With the advent of modern computing, and ever more powerful hardware, it has recently become more and more feasible to solve ever more complex sets of equations using computers.

There exist many numerical codes that are specialized in solving the MHD equations, each with their own set of benefits and drawbacks. A few examples include the STAGGER-code [29], LARE3d [30], RAMSES-MHD [31], and the code used for the numerical work in this thesis; the PENCIL-code [32].

The PENCIL-code contains several features that make it a very suitable for this specific problem. First of all, the code solves the equations in terms of the Vector potential $\boldsymbol{A}$, given by $\nabla \times \boldsymbol{A} = \boldsymbol{B}$. In this way the solenoidal condition $\nabla \cdot \boldsymbol{B} = 0$ is maintained. If the magnetic field $\boldsymbol{B}$ is used, numerical errors can accumulate leading to a loss of this condition, and an unphysical magnetic field.

Additionally the PENCIL-code uses sixth-order spatial derivatives, leading to higher precision on even moderately sized computational grids. The differential equations are solved using third order in time with an adaptive time step to keep the error low. Additionally the density is ρ is replaced by the logarithm of the density $\ln(\rho)$.

The equation of motion (equation (1.6)) that is solved by the code is the following:

$$\frac{D\boldsymbol{v}}{Dt} = -c_{\mathrm{s}}^2 \nabla \ln \rho + \boldsymbol{j} \times \boldsymbol{B}/\rho + \mathbf{F}_{\mathrm{visc}}/\rho \tag{1.12}$$

where $\boldsymbol{v}$ is the fluid velocity, $\frac{D}{Dt} \equiv \frac{\partial}{\partial t} + \boldsymbol{v} \cdot \nabla$ is the convective derivative. The magnetic

field and current are calculated from the vector potential $\boldsymbol{A}$ through $\boldsymbol{B} = \nabla \times \boldsymbol{A}$ and $\boldsymbol{j} = \nabla \times \boldsymbol{B}$.

In the previous section we simplified the viscous term by using the following equation $\rho\nu\nabla^2\boldsymbol{v}$. This makes the equation analytically more tractable, but in actuality the viscous force is anisotropic, and should be calculated from the divergence of the stress tensor.

This is indeed what the PENCIL-code does, the viscous force is calculated from:

$$\mathbf{F}_{\text{visc}} = \nabla \cdot 2\nu\rho\mathbf{S}, \tag{1.13}$$

where ν is the kinematic viscosity and $\mathbf{S}$ is the traceless rate of strain tensor $S_{ij} = \frac{1}{2}(\frac{\partial u_i}{\partial x_j} + \frac{\partial u_j}{\partial x_i}) - \frac{1}{3}\delta_{ij}\nabla \cdot \boldsymbol{v}$.

The continuity equation (1.9) needs to be written in terms of the logarithmic density, and gets the following form:

$$\frac{D \ln \rho}{Dt} = -\nabla \cdot \boldsymbol{v}. \tag{1.14}$$

The last equation to be solved is the induction equation (1.8). By taking the inverse curl on both sides we get the equation in terms of the vector potential, which becomes:

$$\frac{\partial \mathbf{A}}{\partial t} = \boldsymbol{v} \times \mathbf{B} + \eta\nabla^2\mathbf{A} \tag{1.15}$$

where η is the magnetic diffusivity. This particular evolution of $\boldsymbol{A}$ corresponds to using the Weyl gauge, such that $\nabla\phi = 0$ where ϕ is the scalar potential.

These are the equations that are solved using the PENCIL-code. The code contains many more modules, including an entropy to include temperature effects, hyperviscosity, radiation, and gravity, making it an extremely versatile solver, often used for problems in the astrophysical context.

1.4 Helicity

A readers first encounter with the title of this thesis, 'Knots in plasma' might elicit a reaction of surprise; What could these two topics possibly have in common? The answer, quite simply, is the concept of magnetic helicity. In this section we give a historical account, from discovery of a conserved quantity by Woltjer to its topological interpretation and naming by Moffatt and Arnold. We also describe a curious analogy between magnetic helicity and fluid helicity.

In 1958 Woltjer made a curious discovery, namely that in ideal MHD the following integral was a constant of motion [11]:

$$H_{\text{m}} = \int \boldsymbol{B} \cdot \boldsymbol{A} \mathrm{d}^3x. \tag{1.16}$$

An ideal plasma is governed by the equations (1.3) (1.1) and (1.5).

If we calculate the time derivative of the magnetic helicity in a volume V (following the derivation in [33]), we can write it as:

$$\frac{\partial H_\mathrm{m}}{\partial t} = \int_V \frac{\partial \boldsymbol{A}}{\partial t} \cdot \boldsymbol{B} + \boldsymbol{A} \cdot \frac{\partial \boldsymbol{B}}{\partial t} \mathrm{d}^3 x \tag{1.17}$$

$$= \int_V \boldsymbol{A} \cdot \nabla \times (\boldsymbol{v} \times \boldsymbol{B}) \mathrm{d}^3 x \tag{1.18}$$

$$= \int_V -\nabla \cdot (\boldsymbol{A} \times (\boldsymbol{v} \times \boldsymbol{B})) + (\boldsymbol{v} \times \boldsymbol{B} \cdot \nabla \times \boldsymbol{A}) \, \mathrm{d}^3 x \tag{1.19}$$

$$= \oint_{\partial V} ((\boldsymbol{A} \cdot \boldsymbol{v})\boldsymbol{B} - (\boldsymbol{A} \cdot \boldsymbol{B})\boldsymbol{v}) \cdot \mathrm{d}\mathbf{n} \tag{1.20}$$

For equation (1.18) we have used the fact that $\frac{\partial \boldsymbol{A}}{\partial t} \cdot \boldsymbol{B} = 0$, which is seen when the induction equation (1.3) is written in terms of the vector potential (equation (1.15) with $\eta = 0$). The second term in equation (1.19) vanishes because $\boldsymbol{v} \times \boldsymbol{B} \cdot \nabla \times \boldsymbol{A} = \boldsymbol{v} \times \boldsymbol{B} \cdot \boldsymbol{B} = 0$. For the final equation we have used Gauss' theorem to write the volume integral over V into the integral over its surface ∂V, and integrate over the surface normal $\mathbf{n}$.

From this we can see that the time derivative vanishes for any volume on which $\boldsymbol{B} \cdot \mathbf{n} = 0$ and $\boldsymbol{v} \cdot \mathbf{n} = 0$. An example of a surface where $\boldsymbol{B} \cdot \mathbf{n} = 0$ is a flux tube. If we choose a surface that moves with the plasma fluid, the helicity in this flux tube will remain unchanged. In some situations we can also choose a surface sufficiently far away such that $\boldsymbol{B} = 0$ and $\boldsymbol{v} = 0$ on that surface, and the helicity in this volume must remain constant.

In 1969 H. K. Moffatt named this quantity magnetic helicity. The name helicity was chosen in analogy to the concept of helicity in particle physics, the dot product of the spin of a particle with the direction of motion. Since spin is the rotational motion of a particle, its generalization to an extended field is the curl, or rotation of that field.

Moffatt also gave a neat topological interpretation of the concept of helicity: it measures the self- and interlinking of magnetic field lines in the configuration. That helicity measures linking, can be seen by calculating the helicity of a simple configuration of two linked flux tubes, shown in figure 1.3. The configuration consists of two untwisted tubes, carrying magnetic flux Φ_1 and Φ_2 respectively, and the magnetic field is zero outside of the two tubes. The helicity integral (1.16) can then be calculated analytically. Since $\boldsymbol{B} = 0$ outside of the rings, the integral needs only to be carried out over the two separate rings. Since we integrate in the direction of the $\boldsymbol{B}$-field, the integral over a cross-sectional area s_i of the ring $\int_{s_i} B \cdot \mathrm{d}\mathbf{a} = \Phi_i$, and what is left is only the integral in the direction of the ring:

$$H_\mathrm{m} = \Phi_1 \oint_{C_1} \boldsymbol{A} \cdot \mathrm{d}\mathbf{l} + \Phi_2 \oint_{C_2} \boldsymbol{A} \cdot \mathrm{d}\mathbf{l}. \tag{1.21}$$

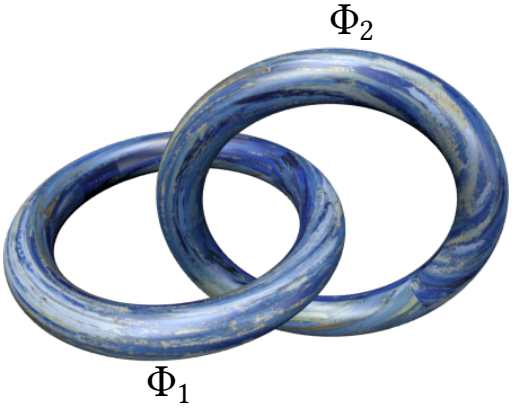

Figure 1.3: Configuration consisting of two linked magnetic rings carrying flux Φ_1 and Φ_2.

Note that this can only be done for a flux tube with no twist.

Since $\boldsymbol{B} = \nabla \times \boldsymbol{A}$, and using Stokes theorem to relate the integral of the vector potential along the boundary with its curl through the surface, we get:

$$H_\mathrm{m} = \Phi_1 \int_{S_1} \boldsymbol{B} \cdot \mathrm{da} + \Phi_2 \int_{S_2} \boldsymbol{B} \cdot \mathrm{da}. \tag{1.22}$$

where S_i is the surface enclosed by the curve C_i. But what is the flux passing through the curve C_i? This is exactly the flux of carried by the other magnetic ring! The total helicity of the configuration thus becomes:

$$H_\mathrm{m} = \Phi_1\Phi_2 + \Phi_2\Phi_1 = 2\Phi_1\Phi_2. \tag{1.23}$$

The above example consists of the mathematically simplest linking, rings that are linked once, but from the derivation we can also deduce what would happen if the curves are non-trivially linked. The integral in equation (1.22) resolves to the amount of flux that passes through the surface enclosed by the curve. If the two curves are linked n times with each other, the flux tube passes through the surface enclosed exactly n times as well, and thus the helicity is proportional to the *linking* number of the two curves.

This interpretation of Helicity as the linking number of the curves goes deeper than

just the toy model presented above. In fact, as we will show in the next section, the helicity integral (1.16) is equivalent to the gauss linking integral calculated over all pairs of field lines in the configuration [12,14].

In the above derivation the assumption was made that the field could be decomposed into distinct flux tubes, all closed curves. In reality this is almost never the case. The solenoidal condition $\nabla \cdot \boldsymbol{B} = 0$ does imply that a field line cannot start or end*, but field lines can be chaotic, filling an entire region of space, or lie on the surface of a torus and fill it ergodically. It was Arnold who introduced the asymptotic Hopf invariant, a measure for the linking of such unclosed field lines, and made the connection between the linking integral and the helicity integral mathematically exact [15].

Magnetic helicity thus has a topological interpretation, namely it measures the linking of the field lines in the plasma. There is also another way to intuitively understand the conservation of helicity. The ideal induction equation (1.3) implies that field lines 'go with the flow'. If there is magnetic flux passing through a perfectly conducting fluid element, any change of this flux will set up a current in the conductor to counteract this change. In the limit of perfect conductivity, the flux through a fluid element cannot change, and the magnetic flux is 'frozen in' to the plasma. If the fluid moves, it drags the magnetic field lines with it. Any fluid flow is thus a deformation of the initial magnetic field, deformed by the fluid displacement. Since this displacement is continuous, all that can happen is that the field lines change shape, but topological invariants such as linking and knotting are not affected. Therefore, since magnetic helicity quantifies this linking and knotting, it will remain unchanged.

1.4.1 Helicity as linking, writhe and twist

Here we will show how the helicity integral (1.16) can be reduced to the gauss linking integral over all pairs of field lines. The Gauss linking integral was first defined by Gauss in the 1833 to calculate the linking number of two closed curves, with his original motivation presumably being to calculate the linking of orbital trajectories [34]. The linking of two closed curves $C_1 = \boldsymbol{r}(x)$ and $C_2 = \boldsymbol{r}'(x')$ is given by:

$$L_{12} = -\frac{1}{4\pi} \oint_{C_1} \oint_{C_2} \frac{\mathrm{d}\boldsymbol{r}}{\mathrm{d}x} \cdot \frac{\boldsymbol{\imath}}{|\boldsymbol{\imath}|^3} \times \frac{\mathrm{d}\boldsymbol{r}'}{\mathrm{d}x'} \mathrm{d}x \mathrm{d}x'. \tag{1.24}$$

Here $\boldsymbol{\imath} = \boldsymbol{r}' - \boldsymbol{r}$ is a vector from one curve to the other.

To reduce the helicity integral (1.16) to this form, we first need to choose a vector potential. Since the vector potential is given by $\boldsymbol{B} = \nabla \times \boldsymbol{A}$, we can uncurl it using a

* Also this is an imprecise statement, more correct would be to state that only a zero-measure subset of field lines can start or end, at null points in the field.

Biot-Savart type integral:

$$\boldsymbol{A}(\boldsymbol{r}) = -\frac{1}{4\pi}\int \frac{\boldsymbol{\wr}}{|\boldsymbol{\wr}|^3} \times \boldsymbol{B}(\boldsymbol{r}')\mathrm{d}^3 r'. \tag{1.25}$$

the helicity integral then becomes:

$$H_{\mathrm{M}} = -\frac{1}{4\pi}\int\int \boldsymbol{B}(x)\cdot\frac{\boldsymbol{\wr}}{|\boldsymbol{\wr}|^3} \times \boldsymbol{B}(x')\mathrm{d}^3 x\mathrm{d}^3 x'. \tag{1.26}$$

The last step is to split up the magnetic field into N distinct flux tubes, each carrying a flux Φ_i and parametrized by curve $C_i = \boldsymbol{r}(x)$. Integration over the entire volume can then be written as sum of the integration over each of these curves individually multiplied by the flux. The helicity then becomes:

$$H_{\mathrm{M}} = -\sum_{i=1}^{N}\sum_{j=1}^{N}\frac{1}{4\pi}\Phi_i\Phi_j \oint_{C_i}\oint_{C_j} \boldsymbol{r}(x)\cdot\frac{\boldsymbol{\wr}}{|\boldsymbol{\wr}|^3} \times \boldsymbol{r}'(x')\mathrm{d}x\mathrm{d}x' = \sum_{i=1}^{N}\sum_{j=1}^{N} L_{ij}\Phi_i\Phi_j. \tag{1.27}$$

The magnetic helicity is thus equal to the flux-weighted sum of all linking numbers. This derivation hinges on the premise that the field can indeed be split up into N distinct closed tubes. This is rarely the case. Field lines can for example be chaotic, ergodically filling an entire region of space, or lying on the surface of of a torus, but still never closing on themselves. For this Arnold introduced the asymptotic Hopf invariant, the result of this linking integral in the asymptotic limit of unclosed field lines [15].

When $i \neq j$ the linking integral just reduces to the integer number of times that curve C_i is linked with curve C_j, but it is especially interesting to look at what this integral evaluates to when $i = j$.

It was shown by Moffatt and Ricca that in this situation the self-helicity of such a tube is equal to the writhe $\mathcal{W}$ and twist Tw of the tube. The writhe corresponds to the curved motion of the centerline of the tube, and twist corresponds to the rotation of the tube itself around its centerline. It was shown by Călugăreanu that the twist and writhe of a curve are two sides of the same coin [35]: the twist and writhe can be translated into each other, but their sum remains constant:

$$L_{ii} = Tw + \mathcal{W} \tag{1.28}$$

This conserved quantity is also sometimes attributed to White [36].

The interplay between helicity as linking, twist and writhe can be demonstrated just using your hands, as shown in figure 1.4. First, form two linked rings using thumb and index finger. These two curves are definitely linked. Now connect your index finger to your index finger, and your thumb to your thumb, to create a single curve. The linking is now gone, but the fingers form a kinked path, writhing in space. The value of the

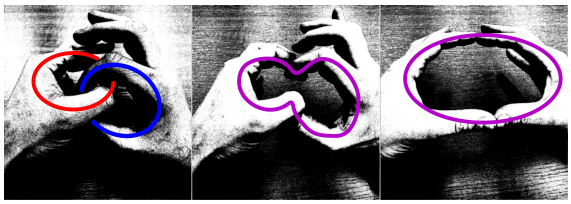

Figure 1.4: The interplay between linking, writhe and twist can easily be seen through a simple experiment: make two linked rings from your fingers. When you 'reconnect' them by touching thumb to thumb, the global configuration has not changed much, but the linking has. Instead, your fingers now form a writhing curve. As you slide your fingers to a circle, you can feel them twist against each other, thus translating writhe into twist.

self-integral evaluated over this single curve is the same as the linking integral over the two curves. Now when you straighten the curve, you will feel the tips of your thumb and index finger twisting against each other. This is the writhe of the curve being translated into twist.

1.4.2 Fluid and magnetic helicity, a comparison

There exists a very interesting parallel between magnetic helicity as defined in equation (1.16), and what is called fluid helicity, which is calculated by the following integral:

$$H_{\mathrm{fl}} = \int \boldsymbol{v} \cdot \omega \mathrm{d}^3 x. \tag{1.29}$$

Here $\omega = \nabla \times \boldsymbol{v}$ is called the vorticity field of the fluid. This equation is mathematically identical to the magnetic helicity integral, with ω taking the place of $\boldsymbol{B}$ and $\boldsymbol{v}$ taking the place of $\boldsymbol{A}$.

Our interpretation of magnetic helicity as linking of field lines is directly translated to fluid helicity, which is now a measure of linking of *vorticity lines*.

Fluid helicity behaves somewhat differently from magnetic helicity. In fact, the equation governing a fluid flow is mathematically simpler than the coupled differential equations governing MHD. The time evolution of an ideal, incompressible fluid is given by the Navier-Stokes equation:

$$\rho\left(\frac{\partial \boldsymbol{v}}{\partial t} + \boldsymbol{v} \cdot \nabla \boldsymbol{v}\right) = \nu \nabla^2 \boldsymbol{v} - \nabla p. \tag{1.30}$$

This equation is equivalent to the momentum equation (1.6), but without the Lorentz force.

Taking the curl of this equation, we can derive the time evolution of vorticity:

$$\frac{\partial \omega}{\partial t} = \nabla \times (\boldsymbol{v} \times \omega) + \nu \nabla^2 \omega. \tag{1.31}$$

Here we have used the fact that $\boldsymbol{v} \cdot \nabla \boldsymbol{v} = \nabla v^2/2 - \boldsymbol{v} \times (\nabla \times \boldsymbol{v})$ (using the same vector identities as in 1.2.3), and the identity $\nabla \times \nabla f = 0$ for any scalar field f, as well as the vector identity $\nabla \times (\nabla^2 \boldsymbol{a}) = \nabla^2 (\nabla \times \boldsymbol{a})$.

In the limit of $\nu \longrightarrow 0$ this condition is identical to the condition on the time evolution of the magnetic field, therefore, vortex lines in an ideal fluid are also 'frozen in', and the vorticity field 'goes with the flow'.

A key difference however is that the magnetic field and the flow field are decoupled in MHD equations. Since the vorticity is directly calculated from the fluid flow through $\omega = \nabla \times \boldsymbol{v}$, any finite vorticity implies a fluid flow around the vortex lines. Consider the simplest case of a single vortex ring parametrized by the curve C. Because the vorticity is zero everywhere outside the vortex ring, the fluid field can be calculated using the Biot-Savart integral:

$$\boldsymbol{v}(\boldsymbol{r}) = -\frac{1}{4\pi} \oint_C \frac{\boldsymbol{r}'}{|\boldsymbol{r}'|^3} \times \boldsymbol{\omega} \mathrm{d}l. \tag{1.32}$$

As we know from the analogous problem of the magnetic field of a current carrying ring, the fluid velocity at any point on the curve C is nonzero. Since we have seen that vorticity 'goes with the flow" any configuration of vortex lines must necessarily be in motion. This is very often seen in nature, as the simple model is actually a very appropriate description of a smoke ring. Smoke rings are therefore always in motion, propelled by the fluid velocity that generates the vorticity field and held together by the conservation of fluid helicity.

In a recent and beautiful experiment Kleckner et al. were able to generate vortex filaments in a laboratory setup with a non-trivial vortex topology [37]. These knotted vortex filaments at first glance seemed to break helicity conservation, as for example a self-linked trefoil filament is immediately seen to fall apart into unlinked simple loops. Upon closer inspection this was not true, because, identical to what we show in section 1.4.1 also fluid helicity can be decomposed into its kinking, writhe and twist components. The initial vortex knot, starting out with only self-linking of vortex filaments, translates this helicity through localized reconnections, which are isolated only to regions where vortex filaments come very close. After a reconnection event, the vortex line is strongly kinked, i.e. it traces a helical path through space, and eventually the helicity is translated to only twist in the vortex lines themselves [38].

different steady states

The analogy between fluid helicity and magnetic helicity is a very interesting one, and both research fields experience a large degree of cross-fertilization because of the mathematical connections between the two concepts. The correspondence however is far from perfect, and especially breaks down when equilibria or steady-state solutions are concerned. Even though both helicities are conserved* under the dynamics of the equations that govern their time evolution, the nature of this evolution is very different.

In section 1.2.3 we described how the Lorentz force can be decomposed into magnetic pressure and magnetic tension. These forces determine the stationary equilibrium that can be obtained.

There are no analogous forces acting on a vortex line, as we can see from equation (1.31), there is merely a term which convects the vorticity with the fluid velocity and a term that acts as a diffusion, causing localized vorticity to diffuse outwards.

1.5 Mathematics of linking: The Hopf map and knot theory

In the previous section we saw how magnetic helicity, or linking of magnetic field lines, is conserved in ideal magnetohydrodynamics. This is a good reason to look at he mathematics of linking, and look at structures that exhibit a high degree of linking, the Hopf fibration.

1.5.1 The Hopf map

In 1931 German mathematician Heinz Hopf published a paper that shook the mathematical field of Topology: He presented a *non-null homotopic map* from the hypersphere S^3 to the normal sphere S^2. The rest of the world barely took notice, and went on with their daily life. Now, nearly a century later, the structure he described is becoming a avidly used tool in theoretical physics.

So what was it that Hopf discovered? Let us first discuss the mathematical concepts used above. The sphere S^2 is just that, a spherical shell. One mathematical way to describe it is the collection of points in space that are all equidistant from the origin; $S^2 \simeq (x, y, z) \in \mathbb{R}^3 | x^2 + y^2 + z^2 = 1$. Here the symbol $\simeq$ denotes that S^2 is *homeomorphic* to that collection of points in three-space. In Topology the exact shape of the object is not important, Hopf's statement works for any sphere, no matter what shape it has. When one wants derive anything from this, it does help to choose a simple parametrization like the one given above.

* Approximately in the resistive case.

The Hypersphere S^3 is a one dimension higher generalization of the sphere, its surface is three-dimensional*. There are several ways of representing S^3, and a simple one is to consider it embedded in the four-dimensional space $\mathbb{C}^2$

$$S^3 \simeq \left\{(z_1, z_2) \in \mathbb{C}^2 \;\middle|\; |z_1|^2 + |z_2|^2 = 1\right\}. \tag{1.33}$$

A map $g : X \longrightarrow Y$ is called null-homotopic if it is homotopic to a constant map, that is to say, that it can be deformed (continuously) to a map that sends all the points in topological space X to a single point in space Y. That the map Hopf described is not null-homotopic means that there is additional structure in the map such that it can not be deformed to this simple form. Let us illustrate this by looking at the Hopf map.

We need to construct a map $h : S^3 \longrightarrow S^2$, using the above description of S^3. Every element (z_1, z_2) should go to to an element of S^2. One thing we can do is divide the two complex numbers, $(z_1, z_2) \longrightarrow \frac{z_1}{z_2}$, which gives us an element in $\mathbb{C}$. There is then a simple method of sending every element of $\mathbb{C}$ to an element of S^2, which is inverse *stereographic projection*, denoted as $\pi^{(2)^{-1}} : \mathbb{C} \cup \infty \longrightarrow S^2$. It can be given by the following operation

$$\pi^{(2)^{-1}} : (a + ib) \longrightarrow \left(\frac{2a}{\not{r}^2 + 1}, \frac{2b}{\not{r}^2 + 1}, \frac{\not{r}^2 - 1}{\not{r}^2 + 1}\right) \tag{1.34}$$

where $\not{r}^2 = a^2 + b^2$.

Regardless of the form we write the stereographic projection in, it is a continuous function, and since the combination of two continuous functions also yields a continuous function, we can write the Hopf map as follows:

$$h : S^3 \longrightarrow S^2 : (z_1, z_2) \longrightarrow \pi^{(2)^{-1}}\left(\frac{z_1}{z_2}\right). \tag{1.35}$$

This has all the properties necessary, it is a map from S^3 to S^2. So what is so special about it? Lets look at how the map sends elements of S^3 to elements of S^2. If we choose an element (z_1, z_2) on S^3, this point goes to a point p on S^2, but that is not the only element of S^3 to go to p. It is easy to see that the point $(z_1 e^{i\theta}, z_2 e^{i\theta})$ also goes to the same point p! It is simple to see that $(z_1 e^{i\theta}, z_2 e^{i\theta}) \in S^3$. There is thus a whole set of points in S^3 that all map to the same point on S^2, which we call the *fiber* f over the point p: $f(p) = \{(w_1, w_2) \in S^3 | w_1 = z_1 e^{i\theta}, w_2 = z_2 e^{i\theta},\ 0 < \theta \leq 2\pi\}$. From this we can already see one beautiful result, every fiber of the Hopf map is a circle! Additionally, every single fiber of the map is linked with every other one. It is this property that makes the map non-null homotopic.

We can construct a vector field in $\mathbb{R}^3$ by extending the Hopf map to a map from $\mathbb{R}^3$

* In fact S^n describes a topological object that is homeomorphic to the set of points in $\mathbb{R}^{n+1}$ that is equidistant to the origin, for example S^1 is a circle, the set of points in 2d space all distance 1 from the origin.

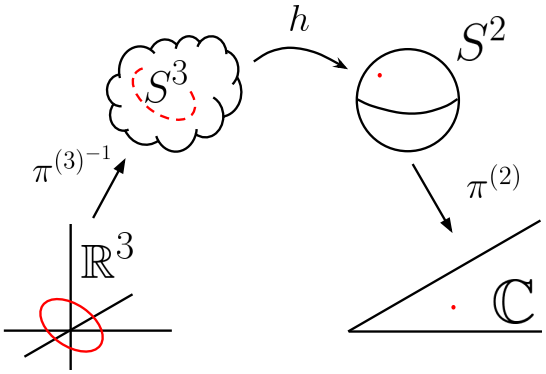

Figure 1.5: Graphical representation of the construction of the function ϕ used to generate a vector field everywhere tangent to fibers of the Hopf map.

to $\mathbb{C}$. This construction is illustrated in figure 1.5 and consists of using the Hopf map to construct a function from $\mathbb{R}^3$ to $\mathbb{C}$ in the following way:

$$\phi : \mathbb{R}^3 \longrightarrow \mathbb{C}, \ \phi = \pi^{(2)} \circ h \circ \pi^{(3)^{-1}}, \tag{1.36}$$

with $\pi^{(3)^{-1}} : \mathbb{R}^3 \longrightarrow S^3$ inverse stereographic projection (from the north pole of S^3) to the three-sphere. When we fill in the correct functions for stereographic projection this map has the following explicit form:

$$\phi(x, y, z) = \frac{(2(x + iy))}{\left(2z + i(r^2 - 1)\right)}, \tag{1.37}$$

where $r^2 = x^2 + y^2 + z^2$. We get a vector field in $\mathbb{R}^3$, which we will preemptively call B and give correct dimensions, by calculating

$$\mathbf{B} = \frac{\sqrt{a}}{2\pi i} \frac{\nabla\phi \times \nabla\phi^*}{(1 + \phi\phi^*)^2}. \tag{1.38}$$

Here $\sqrt{a}$ is the constant such that the magnetic field has correct dimensions. The cross product between $\nabla\phi$ and $\nabla\phi^*$ is a vector in the direction that ϕ remains constant, i.e. a vector in the direction of the circles of the Hopf map.

The result of the calculation is the following simple analytical expression:

$$\mathbf{B} = \frac{4\sqrt{a}}{\pi(1+r^2)^3}\begin{pmatrix} 2(y-xz) \\ -2(x+yz) \\ (-1+x^2+y^2-z^2) \end{pmatrix}. \tag{1.39}$$

Since, by construction the magnetic field is always in the direction of the fibers of the Hopf map, and stereographic projection maps circles to circles, the magnetic field direction is at any point in space tangent to one of the fibers of the map. In other words, every single field line of this field is a perfect circle, and every single field line is linked with every other one.

We can adapt the Hopf map such that the fibers are not just circles but any torus knot. This was done by Arrayás and Trueba in their recent paper [21] in the following way:

$$h^{(\omega_1,\omega_2)} := \pi^{(2)^{-1}}\left(\frac{z_1^{(\omega_2)}}{z_2^{(\omega_1)}}\right). \tag{1.40}$$

Here $z^{(w)}$ indicates the operation on a complex number such that only its argument is multiplied by the real number w. From this definition follows that $h^{(\omega_1,\omega_2)}(z_1, z_2) = h^{(\omega_1,\omega_2)}(e^{i\omega_1\theta}z_1, e^{i\omega_2\theta}z_2)$ for all values of θ. Consequently the pre-image of a point on S^2 is a continuous curve in S^3. If $\omega_1 = \omega_2$ each curve is again a circle in S^3, and the map is identical to the Hopf map up to a pre-factor. For $\omega_1 \neq \omega_2$ the pre-image of a point in S^2 is a curve in S^3 that oscillates in the z_1-direction with frequency ω_1 and in the z_2-direction with frequency ω_2.

The construction of a vector field is done in the same way as equation (1.37). The function ϕ becomes:

$$\phi(x,y,z) = \frac{(2(x+iy))^{(\omega_2)}}{\left(2z+i(r^2-1)\right)^{(\omega_1)}}, \tag{1.41}$$

The curves of constant ϕ are continuous, oscillating and closed (or, for incommensurate ω_1 and ω_2, dense in a compact subspace of S^3) curves in S^3, and will thus be so too in $\mathbb{R}^3 \cup \infty$.

In order to scale the field to any desired size r_0 we use the substitution $(x,y,z) \longrightarrow \left(\frac{x}{r_0}, \frac{y}{r_0}, \frac{z}{r_0}\right)$ to obtain the expression for a magnetic field:

$$\mathbf{B} = \frac{4r_0^4\sqrt{a}}{\pi(r_0^2+r^2)^3}\begin{pmatrix} 2(\omega_2 r_0 y - \omega_1 xz) \\ -2(\omega_2 r_0 x + \omega_1 yz) \\ \omega_1(-r_0^2+x^2+y^2-z^2) \end{pmatrix}. \tag{1.42}$$

This field is cylindrically symmetric as can be seen by the absence of a θ-dependence

when equation (1.42) is put in cylindrical coordinates:

$$\mathbf{B}(r,\theta,z) = \frac{4r_0^2\sqrt{a}}{\pi\left(r_0^2+r^2+z^2\right)^3}(-2\omega_2 r_0 r\hat{\theta} - 2\omega_1 z r\hat{r} + \omega_1(-r_0^2+r^2-z^2)\hat{z}). \tag{1.43}$$

Every field line lies on the surface of a member of a set of nested tori. The smallest reduces to a circle with radius of r_0 (magnetic axis), and the largest is a line along the z-axis. The field lines wind around the poloidal direction with frequency ω_1, and toroidal direction with frequency ω_2. If $\frac{\omega_1}{\omega_2}$ is rational, $\frac{\omega_1}{\omega_2} = \frac{n}{m}$, and every field line is a (n, m) torus knot. We stress that every integral curve of this field is itself a knot (or circle, or ergodically spanning the toroidal surface), but the global field is smooth and continuous. The ratio $\frac{\omega_1}{\omega_2}$ gives the ratio of toroidal to poloidal winding of the curves also called the rotational transform ι.

helicity and magnetic energy of these fields

The vector potential corresponding with the field in equation (1.42) is given by

$$\mathbf{A} = \frac{r_0^3\sqrt{a}}{\pi(r_0^2+r^2)^2}\begin{pmatrix} 2(r_0\omega_1 y - \omega_2 xz) \\ -2(r_0\omega_1 x + \omega_2 yz) \\ \omega_2(-r_0^2+x^2+y^2-z^2)\end{pmatrix}. \tag{1.44}$$

The inner product $\mathbf{A}\cdot\mathbf{B}$ is given by

$$\mathbf{A}\cdot\mathbf{B} = \frac{4ar_0^7\omega_1\omega_2}{\pi^2(r_0^2+r^2)^3}. \tag{1.45}$$

The helicity is then

$$H_\mathrm{m} = \int \frac{4ar_0^7\omega_1\omega_2}{\pi^2(r_0^2+r^2)^3}\,\mathrm{d}^3x = ar_0^4\omega_1\omega_2. \tag{1.46}$$

The value of B^2 is given by

$$\mathbf{B}\cdot\mathbf{B} = \frac{16ar_0^8}{\pi^2(r_0^2+r^2)^6}\left(4r_0^2(\omega_2^2-\omega_1^2)(x^2+y^2) + \omega_1^2(r_0^2+r^2)^2\right), \tag{1.47}$$

which allows us to calculate the integral of B^2 over all space

$$\int B^2\,\mathrm{d}^3x = ar_0^3(\omega_1^2+\omega_2^2). \tag{1.48}$$

1.5.2 The Kamchatnov-Hopf soliton

The remarkable structure of the Hopf map was used by Kamchatnov to define an Ideal MHD soliton [17]. A soliton in this sense is an exact and stationary (in time) solution of the ideal incompressible MHD equations*. In a paper titled "On the stability of the simplest solution of the equations of hydromagnetics" Chandrasekhar showed that equations (1.3) and (1.1) can be solved by the following choices of velocity and pressure [39]:

$$\boldsymbol{v} = \pm \frac{\boldsymbol{B}}{\sqrt{\rho}}, \quad p = p_\infty - \frac{B^2}{2}. \tag{1.49}$$

This solution of the equations is also stable against linear perturbations.

Kamchatnov analyzed this solution for the specific case where the velocity field and the magnetic field are given by the Hopf fibration, equation (1.39). In his derivation Kamchatnov used a different mathematical method than we presented above. He used the pull-back via the Hopf map of the two-form on S^2 to S^3, and stereographic projection to $\mathbb{R}^3$ to calculate the magnetic field, but the analytical expression he derived is identical.

1.6 This thesis

In this thesis we study magnetic topology, the linking and knotting, and the structures formed by and of magnetic field lines in plasma employing numerical and analytical methods. Of central importance is the self-organization of plasma into these structures when numerical dissipation is included. Specifically, this thesis is organized into the following sections:

- **Chapter 2** (*Self-organizing Knotted Magnetic Structures in Plasma*) shows that linking in a magnetic configuration gives rise to self-organizing toroidal magnetic structures when the field is allowed to relax with a finite resistivity. The initial helicity is provided by a configuration consisting of a finite number of linked and/or twisted rings. The attained structure is in a MHD equilibrium, such that the Lorentz force is balanced by the gradient in pressure force. An essential feature of this configuration is a *lowered* pressure on the magnetic axis of the configuration. In these structures the rotational transform is almost constant, such that the fields have similar magnetic topology to the (adapted) Hopf map.
- **Chapter 3** (*Ideal relaxation of the Hopf fibration*) looks into the equilibrium attained by a topologically nontrivial field using an ideal (zero-resistance) relaxation

* The term soliton is more often used to describe waves in a nonlinear dispersive medium with a constant shape in time. Except for the solutions both being constant in time, these two concepts have little to do with one another.

technique. The initial fields are derived from the Hopf map, and thus have similar magnetic topology to those described in chapter 1. The Lagrangian relaxation method, which evolves the field by distorting the grid, gives a visual representation of how the field needs to be distorted from the initial configuration to attain an MHD equilibrium. Using the virial theorem we show how a finite pressure is necessary for any localized equilibrium to be attainable.

- **Chapter 4** (*On the topology of Magnetic Surfaces in Decaying Plasma Torus Knots*) considers the resistive evolution of plasma torus knots, plasma configurations that are stable topological solitons in ideal magnetohydrodynamics. These finite energy, localized configurations consist of linked and knotted magnetic field lines and toroidal magnetic surfaces, and depending on the poloidal and toroidal integer, specific lines where the magnetic field vanishes. The resistive dynamics give rise to localized reconnections that change the magnetic topology and allow new magnetic surfaces to arise. The intersection of the zero line (present when the poloidal integer is larger than one, and which is stable in time) with the new surfaces gives rise to zero points of the magnetic field on these surfaces, such that through the Hopf-Poincaré index theorem the surface is topologically distinct from a torus.

- **Chapter 5** (*Universal Growth Rate and Helical Reorganization in Self-organizing Knots*) investigates the time evolution of the self-organized equilibrium described in chapter 1. A different initial condition, consisting of a single toroidal flux tube contains the initial helicity. The created structures grow in time due to resistive field line slip against a quasi-static equilibrium. When the ratio of plasma to magnetic pressure exceeds a threshold, the configuration becomes susceptible to a kinking of the magnetic axis, which destroys the initial axisymmetry. The mode numbers of this external kink instability do not have to be equal to any magnetic mode numbers present in the field. Magnetic reconnections in this external kink mode lead to nonaxisymmetric perturbations of the magnetic field. These perturbations give rise to magnetic islands at rational surfaces. At even higher magnetic field strength these perturbations lead to the creation of regions of magnetic chaos.